

Magnetocrystalline anisotropy in ferromagnetic films

M. Cinal* and D. M. Edwards

Department of Mathematics, Imperial College, London SW7 2BZ, United Kingdom

J. Mathon

Department of Mathematics, City University, London EC1V 0HB, United Kingdom

(Received 11 April 1994)

The magnetocrystalline anisotropy (MA) of ferromagnetic fcc Ni, fcc Co, and bcc Fe (001) slabs is calculated to second order in the spin-orbit coupling constant using realistic tight-binding models with parameters fitted to available first-principles electronic-structure calculations. Results for slabs with 1–17 atomic layers show that MA favors magnetization perpendicular to the slab for Fe but in-plane for Ni and Co, in agreement with experiment. Fluctuations in the MA as the thickness is varied indicate that surface MA is not purely of local origin in the surface atomic layer.

I. INTRODUCTION

The dependence of the energy of a ferromagnetic metal on the direction of the magnetic moment, known as the magnetocrystalline anisotropy (MA), becomes especially pronounced at the surface or in thin films as was predicted by Néel¹ in 1954. Due to potential applications in magnetic perpendicular recording, this effect has recently received much attention from experimentalists.^{2–12} On the other hand, there are still only a few theoretical calculations of the surface MA (SMA). As proposed by Van Vleck in 1937,¹³ the source of MA is spin-orbit coupling, so it is a relativistic effect. So far two different theoretical approaches have been applied to the problem of SMA. One method involves *ab initio* calculations with spin-orbit interaction included and determination of total energies for different spin orientations.^{14–20} These calculations are however associated with very extensive numerical computations. The other method uses the fact that the spin-orbit interaction is small compared to characteristic energies of the system (e.g., the bandwidth) which makes a perturbation treatment possible. This approach implemented in the tight-binding framework was adopted in the two earliest papers on SMA.^{21,22} These papers, however, oversimplify the band structure and give only a reasonable order of the magnitude of the effect. On the other hand, a recent paper by Bruno,²³ following similar lines (but using a more realistic band structure), supplied predictions of SMA which agree qualitatively with the *ab initio* results. However, his work was restricted to unsupported monolayers.

The perturbation-theory tight-binding approach has also been applied in the present paper. In the first part of our work (Sec. III A) we study the influence of the surface crystal-field splitting between the in-plane and out-of-plane *d* orbitals and of the *sp-d* hybridization on MA in the (001) fcc nickel monolayer. The main part of the paper (Sec. III B) focuses on examining MA in ferromagnetic slabs of fcc nickel, fcc cobalt, and bcc iron. We study the dependence of MA on the slab thickness (up to 17 layers) with the objective of determining how many layers contribute to the MA of a ferromagnetic surface.

II. THEORY

Ferromagnetic films are described in the slab geometry by implementing the standard Slater-Koster tight-binding formalism.^{24,25} The basis functions are orthonormalized atomic orbitals $|jl\mu\sigma\rangle$ where *j* and *l* label the *j*th atom in the *l*th layer, μ denotes an atomic orbital (i.e., one of the 3*d* orbitals: *xy*, *yz*, *zx*, x^2-y^2 , $3r^2-z^2$, and also, when used, the 4*s* orbital or one of the 4*p* orbitals: *x*, *y*, *z*; the *z* axis being chosen perpendicular to the slab), σ is the spin ($=\uparrow, \downarrow$). Then we introduce the in-plane functions

$$|\mathbf{k}l\mu\sigma\rangle = N^{-1/2} \sum_j \exp(i\mathbf{k}\cdot\mathbf{R}_j^{(l)}) |jl\mu\sigma\rangle, \quad (1)$$

where $\mathbf{R}_j^{(l)}$ is the position of an atom in the *xy* plane of the *l*th layer, \mathbf{k} is a two-dimensional wave vector, *N* is the number of atoms in each layer. The eigenstates

$$|n\mathbf{k}\sigma\rangle = \sum_{l\mu} a_{n,l\mu}^\sigma(\mathbf{k}) |\mathbf{k}l\mu\sigma\rangle \quad (2)$$

and the corresponding eigenenergies $\epsilon_{n\sigma}(\mathbf{k})$ can be found for each spin σ by solving the matrix eigenequation

$$\sum_{l'\nu} H_{l\mu,l'\nu}^\sigma(\mathbf{k}) a_{n,l'\nu}^\sigma(\mathbf{k}) = \epsilon_{n\sigma}(\mathbf{k}) a_{n,l\mu}^\sigma(\mathbf{k}). \quad (3)$$

We assume here that, in the absence of spin-orbit coupling, the matrix of the Hamiltonian *H*, defined as

$$H_{l\mu,l'\nu}^\sigma(\mathbf{k}) = \sum_j \langle 0l\mu\sigma | H | jl'\nu\sigma \rangle \exp[i\mathbf{k}\cdot(\mathbf{R}_j^{(l')} - \mathbf{R}_0^{(l)})] \quad (4)$$

depends on the spin σ only through the exchange term $\frac{1}{2}p(\sigma)\Delta_{\text{ex}}^{(l)}\delta_{\mu\nu}\delta_{ll'}$ where $p(\uparrow) = -1$, $p(\downarrow) = 1$. The elements $\langle 0l\mu\sigma | H | jl'\nu\sigma \rangle$ are calculated in the two-center approximation.²⁴

Now we introduce the spin-orbit coupling $\xi\mathbf{L}\cdot\mathbf{S}$ assumed to be present only on the same site:

$$\begin{aligned} H_{\text{so}} &= \xi \sum_{jl} \sum_{\mu\nu} \sum_{\sigma\sigma'} \langle \mu\sigma | \mathbf{L}\cdot\mathbf{S} | \nu\sigma' \rangle c_{jl\mu\sigma}^+ c_{jl\nu\sigma'} \\ &= \xi \sum_{\mathbf{k}} \sum_l \sum_{\mu\nu} \sum_{\sigma\sigma'} \langle \mu\sigma | \mathbf{L}\cdot\mathbf{S} | \nu\sigma' \rangle c_{l\mu\sigma}^+(\mathbf{k}) c_{l\nu\sigma'}(\mathbf{k}), \end{aligned} \quad (5)$$

where c^+ and c are creation and annihilation operators, respectively. When the direction of the spin \mathbf{S} is along an arbitrary \bar{z} axis characterized by the standard angles θ and ϕ (i.e., $S_z|\sigma\rangle = -\frac{1}{2}\hbar p(\sigma)|\sigma\rangle$), the matrix elements $\langle\mu\sigma|\mathbf{L}\cdot\mathbf{S}|\nu\sigma'\rangle$ depend on these angles. For d orbitals these dependencies are given in Ref. 26; for a general case they can be found with the expressions given in the Appendix of Ref. 16.

Treating H_{so} as a perturbation, we find that the first-order correction $\langle\Phi_0|H_{so}|\Phi_0\rangle$ to the energy E_0 of the groundstate $|\Phi_0\rangle = \prod_{\mathbf{k}n\sigma}\eta[\epsilon_F - \epsilon_{n\sigma}(\mathbf{k})]c_{n\sigma}^+(\mathbf{k})|0\rangle$ vanishes due to symmetry; here ϵ_F is the Fermi energy and $\eta(x)$ is the unit step function. This is quite obvious if one notices that the matrix elements $\langle\mu\sigma|\mathbf{L}\cdot\mathbf{S}|\nu\sigma\rangle$ contain only terms proportional to $\cos\theta$, $\sin\theta\cos\phi$, $\sin\theta\sin\phi$. The second-order correction

$$E^{(2)} = \sum_{\Phi} \frac{|\langle\Phi|H_{so}|\Phi_0\rangle|^2}{E_0 - E} = -\xi^2 \sum_{\mu_1\mu_2\mu_3\mu_4} \sum_{\sigma'\sigma''} \langle\mu_1\sigma'|\mathbf{L}\cdot\mathbf{S}|\mu_2\sigma''\rangle \langle\mu_3\sigma''|\mathbf{L}\cdot\mathbf{S}|\mu_4\sigma'\rangle \times \sum_{\mathbf{k}} \sum_{n'n''} \frac{1}{\epsilon_{n''\sigma''}(\mathbf{k}) - \epsilon_{n'\sigma'}(\mathbf{k})} \eta[\epsilon_{n''\sigma''}(\mathbf{k}) - \epsilon_F] \eta[\epsilon_F - \epsilon_{n'\sigma'}(\mathbf{k})] \times \sum_{l'l''} a_{n',l'\mu_4}^{\sigma'}(\mathbf{k}) [a_{n',l'\mu_1}^{\sigma'}(\mathbf{k})]^* a_{n'',l''\mu_2}^{\sigma''}(\mathbf{k}) [a_{n'',l''\mu_3}^{\sigma''}(\mathbf{k})]^* \quad (6)$$

is obtained with the excited states $|\Phi\rangle = c_{n''\sigma''}^+(\mathbf{k})c_{n'\sigma'}(\mathbf{k})|\Phi_0\rangle$ having the energy $E = E_0 + \epsilon_{n''\sigma''}(\mathbf{k}) - \epsilon_{n'\sigma'}(\mathbf{k})$, where $\epsilon_{n'\sigma'}(\mathbf{k}) < \epsilon_F < \epsilon_{n''\sigma''}(\mathbf{k})$; no other excited states contribute to $E^{(2)}$. This energy correction is nonzero and, unlike in the bulk cubic case,²⁷ it exhibits an angular dependence. For (001) fcc and (001) bcc slabs considered in our paper, this dependence takes the usual form:

$$\frac{E^{(2)}}{N} = K_0 + K_{\text{anis}} \cos^2\theta. \quad (7)$$

Other terms arising from $\langle\mu_1\sigma'|\mathbf{L}\cdot\mathbf{S}|\mu_2\sigma''\rangle \langle\mu_3\sigma''|\mathbf{L}\cdot\mathbf{S}|\mu_4\sigma'\rangle$ are ruled out by symmetry considerations. The coefficient K_{anis} , called the *anisotropy constant*, determines the anisotropic part of the energy $E^{(2)}/N$ per unit two-dimensional surface cell. Its explicit form, as well as that of K_0 , can be easily found from Eq. (6) by extracting $\cos^2\theta$ terms from the products $\langle\mu_1\sigma'|\mathbf{L}\cdot\mathbf{S}|\mu_2\sigma''\rangle \langle\mu_3\sigma''|\mathbf{L}\cdot\mathbf{S}|\mu_4\sigma'\rangle$ (e.g., with a simple numerical algorithm). The anisotropy constant K_{anis} obtained can be expressed as

$$K_{\text{anis}} = -\xi^2 \sum_{\sigma'\sigma''} \sum_t b_{\mu_1\mu_2\mu_3\mu_4}^{\sigma'\sigma''} F_{\mu_1\mu_2\mu_3\mu_4}^{\sigma'\sigma''}, \quad (8)$$

where

$$F_{\mu_1\mu_2\mu_3\mu_4}^{\sigma'\sigma''} = \text{Re}[J_{\mu_1\mu_2\mu_3\mu_4}^{\sigma'\sigma''} - J_{\mu_2\mu_1\mu_3\mu_4}^{\sigma'\sigma''} - J_{\mu_1\mu_2\mu_4\mu_3}^{\sigma'\sigma''} + J_{\mu_2\mu_1\mu_4\mu_3}^{\sigma'\sigma''}] \quad (9)$$

and

$$J_{\mu_1\mu_2\mu_3\mu_4}^{\sigma'\sigma''} = \frac{1}{N} \sum_{\mathbf{k}} \sum_{n'n''} \frac{1}{\epsilon_{n''\sigma''}(\mathbf{k}) - \epsilon_{n'\sigma'}(\mathbf{k})} \eta[\epsilon_{n''\sigma''}(\mathbf{k}) - \epsilon_F] \eta[\epsilon_F - \epsilon_{n'\sigma'}(\mathbf{k})] \sum_{l'l''} a_{n',l'\mu_4}^{\sigma'}(\mathbf{k}) [a_{n',l'\mu_1}^{\sigma'}(\mathbf{k})]^* a_{n'',l''\mu_2}^{\sigma''}(\mathbf{k}) [a_{n'',l''\mu_3}^{\sigma''}(\mathbf{k})]^*. \quad (10)$$

The values of the indices $\mu_1, \mu_2, \mu_3, \mu_4$ that correspond to the t th coefficient $b_{\mu_1\mu_2\mu_3\mu_4}^{\sigma'\sigma''}$ and the coefficients themselves are given for $\sigma' = \sigma'' = \uparrow$ and $\sigma' = \uparrow, \sigma'' = \downarrow$ in Table I. To find $b_{\mu_1\mu_2\mu_3\mu_4}^{\sigma'\sigma''}$ for $\sigma' = \sigma'' = \downarrow$ and $\sigma' = \downarrow, \sigma'' = \uparrow$ we apply the relations

$$b_{\mu_1\mu_2\mu_3\mu_4}^{\downarrow\downarrow} = b_{\mu_1\mu_2\mu_3\mu_4}^{\uparrow\uparrow}, \quad (11)$$

$$b_{\mu_1\mu_2\mu_3\mu_4}^{\downarrow\uparrow} = b_{\mu_1\mu_2\mu_3\mu_4}^{\uparrow\downarrow}, \quad (12)$$

which are a direct consequence of the general symmetry properties of the matrix elements $\langle\mu\sigma'|\mathbf{L}\cdot\mathbf{S}|\nu\sigma''\rangle$. The coefficients $b_{\mu_1\mu_2\mu_3\mu_4}^{\sigma'\sigma''}$ fulfill also an additional simple rela-

tion

$$b_{\mu_1\mu_2\mu_3\mu_4}^{\uparrow\downarrow} = -b_{\mu_1\mu_2\mu_3\mu_4}^{\downarrow\uparrow}, \quad (13)$$

which can be immediately deduced from Table I. This, combined with relations (11) and (12), allows us to rewrite Eq. (8) as follows:

$$K_{\text{anis}} = -\xi^2 \sum_t b_{\mu_1\mu_2\mu_3\mu_4}^{\uparrow\uparrow} [F_{\mu_1\mu_2\mu_3\mu_4}^{\uparrow\uparrow} - F_{\mu_1\mu_2\mu_3\mu_4}^{\uparrow\downarrow} - F_{\mu_1\mu_2\mu_3\mu_4}^{\downarrow\uparrow} + F_{\mu_1\mu_2\mu_3\mu_4}^{\downarrow\downarrow}]. \quad (14)$$

An expression similar to (8) can be derived also for K_0 :

TABLE I. The coefficients $b_{\mu_1\mu_2\mu_3\mu_4}^{\sigma'\sigma''}$ for $\sigma'=\sigma''=\uparrow$ and $\sigma'=\uparrow, \sigma''=\downarrow$ entering Eq. (8) for K_{anis} . The values 1, 2, ..., 9 of indices $\mu_1, \mu_2, \mu_3, \mu_4$ correspond to the orbitals $xy, yz, zx, x^2-y^2, 3r^2-z^2, s, x, y, z$ in the listed order.

t	μ_1	μ_2	μ_3	μ_4	$b_{\mu_1\mu_2\mu_3\mu_4}^{\uparrow\uparrow}$	$b_{\mu_1\mu_2\mu_3\mu_4}^{\uparrow\downarrow}$
1	1	2	1	2	$\frac{1}{4}$	$-\frac{1}{4}$
2	1	2	3	4	$-\frac{1}{2\sqrt{3}}$	$\frac{1}{2}$
3	1	2	3	5	$\frac{\sqrt{3}}{2}$	$-\frac{1}{\sqrt{3}}$
4	1	2	7	9	$\frac{2}{\sqrt{3}}$	$-\frac{2}{\sqrt{3}}$
5	1	4	1	4	-1	1
6	1	4	2	3	-1	1
7	1	4	7	8	1	-1
8	2	3	2	3	$-\frac{1}{4}$	$\frac{1}{4}$
9	2	3	7	8	$\frac{1}{2}$	$-\frac{1}{2}$
10	3	4	3	4	$\frac{1}{4}$	$-\frac{1}{4}$
11	3	4	3	5	$-\frac{\sqrt{3}}{2}$	$\frac{\sqrt{3}}{2}$
12	3	4	7	9	$-\frac{1}{2}$	$\frac{1}{2}$
13	3	5	3	5	$\frac{3}{4}$	$-\frac{3}{4}$
14	3	5	7	9	$\frac{\sqrt{3}}{2}$	$-\frac{\sqrt{3}}{2}$
15	7	8	7	8	$-\frac{1}{4}$	$\frac{1}{4}$
16	7	9	7	9	$\frac{1}{4}$	$-\frac{1}{4}$

TABLE II. The coefficients $d_{\mu_1\mu_2\mu_3\mu_4}^{\sigma'\sigma''}$ for $\sigma'=\sigma''=\uparrow$ and $\sigma'=\uparrow, \sigma''=\downarrow$ entering Eq. (15) for K_0 . The values 1, 2, ..., 9 of indices $\mu_1, \mu_2, \mu_3, \mu_4$ correspond to the orbitals $xy, yz, zx, x^2-y^2, 3r^2-z^2, s, x, y, z$ in the listed order.

$\sigma'=\sigma''=\uparrow$						$\sigma'=\uparrow, \sigma''=\downarrow$					
t	μ_1	μ_2	μ_3	μ_4	$d_{\mu_1\mu_2\mu_3\mu_4}^{\uparrow\uparrow}$	t	μ_1	μ_2	μ_3	μ_4	$d_{\mu_1\mu_2\mu_3\mu_4}^{\uparrow\downarrow}$
1	1	2	1	2	$-\frac{1}{4}$	1	1	3	1	3	$-\frac{1}{4}$
2	1	2	3	4	$\frac{1}{2}$	2	1	3	2	4	$-\frac{1}{2}$
3	1	2	3	5	$-\frac{\sqrt{3}}{2}$	3	1	3	2	5	$-\frac{\sqrt{3}}{2}$
4	1	2	7	9	$-\frac{1}{2}$	4	1	3	8	9	$-\frac{1}{2}$
5	3	4	3	4	$-\frac{1}{4}$	5	1	4	1	4	-1
6	3	4	3	5	$\frac{\sqrt{3}}{2}$	6	1	4	2	3	-1
7	3	4	7	9	$\frac{1}{2}$	7	1	4	7	8	1
8	3	5	3	5	$-\frac{3}{4}$	8	2	3	2	3	$-\frac{1}{4}$
9	3	5	7	9	$-\frac{\sqrt{3}}{2}$	9	2	3	7	8	$\frac{1}{2}$
10	7	9	7	9	$-\frac{1}{4}$	10	2	4	2	4	$-\frac{1}{4}$
11	2	4	2	5	$-\frac{\sqrt{3}}{2}$	11	2	4	2	5	$-\frac{\sqrt{3}}{2}$
12	2	4	8	9	$-\frac{1}{2}$	12	2	4	8	9	$-\frac{1}{2}$
13	2	5	2	5	$-\frac{3}{4}$	13	2	5	2	5	$-\frac{3}{4}$
14	2	5	8	9	$-\frac{\sqrt{3}}{2}$	14	2	5	8	9	$-\frac{\sqrt{3}}{2}$
15	7	8	7	8	$-\frac{1}{4}$	15	7	8	7	8	$-\frac{1}{4}$
16	8	9	8	9	$-\frac{1}{4}$	16	8	9	8	9	$-\frac{1}{4}$

$$K_0 = -\xi^2 \sum_{\sigma'\sigma''} \sum_t d_{\mu_1\mu_2\mu_3\mu_4}^{\sigma'\sigma''} F_{\mu_1\mu_2\mu_3\mu_4}^{\sigma'\sigma''}, \quad (15)$$

where the indices $\mu_1, \mu_2, \mu_3, \mu_4$ and the coefficients $d_{\mu_1\mu_2\mu_3\mu_4}^{\sigma'\sigma''}$ for $\sigma'=\sigma''=\uparrow$ and $\sigma'=\uparrow, \sigma''=\downarrow$ are in Table II. For $\sigma'=\sigma''=\downarrow$ and $\sigma'=\downarrow, \sigma''=\uparrow$ the sets of indices $\mu_1, \mu_2, \mu_3, \mu_4$ appearing in Eq. (15) are the same as for $\sigma'=\sigma''=\uparrow$ and $\sigma'=\uparrow, \sigma''=\downarrow$, respectively, while the coefficients $d_{\mu_1\mu_2\mu_3\mu_4}^{\downarrow\downarrow}$ and $d_{\mu_1\mu_2\mu_3\mu_4}^{\downarrow\uparrow}$ can be found from the general symmetry relations analogous to Eqs. (11) and (12). However, there is no analog of the relation (13), and, in consequence, of relation (14). For K_0 the number of the coefficients $d_{\mu_1\mu_2\mu_3\mu_4}^{\sigma'\sigma''}$ given in Table II is different for $\sigma'=\sigma''=\uparrow$ and $\sigma'=\uparrow, \sigma''=\downarrow$. Also, the sets of indices $\mu_1, \mu_2, \mu_3, \mu_4$ do not coincide for $\sigma'=\sigma''=\uparrow$ and $\sigma'=\uparrow, \sigma''=\downarrow$ as is the case for K_{anis} (cf. Table I).

Let us note that $E^{(2)}$ given in Eq. (6) is *not* identical with that given by Bruno.²³ In his expression $\langle \mu_1\sigma' | \mathbf{L} \cdot \mathbf{S} | \mu_2\sigma'' \rangle \langle \mu_3\sigma'' | \mathbf{L} \cdot \mathbf{S} | \mu_4\sigma' \rangle$ is replaced by $p(\sigma')p(\sigma'') \langle \mu_1\uparrow | \mathbf{L} \cdot \mathbf{S} | \mu_2\uparrow \rangle \langle \mu_3\uparrow | \mathbf{L} \cdot \mathbf{S} | \mu_4\uparrow \rangle$. Nevertheless, Bruno's expression leads to the same value of K_{anis} since both products have the same $\cos^2\theta$ terms; this is also true for the additional anisotropy constant present in the term proportional to $\sin^2\theta \cos^2\phi$ appearing in (110) fcc slabs. The explicit expression for K_{anis} given in Ref. 23 does not coincide exactly with the one derived here, not only due to neglect of p orbitals in Ref. 23, but mainly because its author uses $\sin^2\theta$ and $\sin^2\theta \cos(2\phi)$, instead of $\cos^2\theta$ and $\sin^2\theta \cos^2\phi$ used here, as independent angular functions. However, for the (001) fcc and (001) bcc slabs, where the $\sin^2\theta \cos^2\phi$ term of $E^{(2)}$ vanishes [and so

does the $\sin^2\theta \cos(2\phi)$ term], both the expressions for K_{anis} provide the same value, though, obviously, of different sign. Let us also note that Bruno's expression for $E^{(2)}$ fails to reproduce the correct K_0 , e.g., it improperly predicts $K_0=0$ for the paramagnetic case. This is due to the neglect of some angular-independent terms in the course of the derivation of $E^{(2)}$ which is presented in detail in Appendix 3 of Ref. 28.

Due to the energy denominator in Eq. (10), K_{anis} is very slowly converging with the number of the \mathbf{k} vectors. To achieve the convergence we apply the triangular method and the variant appropriate to our case is briefly presented in the Appendix.

III. RESULTS

A. (001) fcc nickel unsupported monolayer

In this case we calculate anisotropy constants with and without the $sp-d$ hybridization. The full spd tight-binding scheme for the unsupported nickel monolayer is based on the bulk (orthogonal) fit by Papaconstantopoulos.²⁹ We take into account the first- and second-nearest neighbors and use the bulk values of the off-diagonal two-center integrals. The bulk diagonal parameters are changed to fit to the *ab initio* energy bands for the nickel monolayer:^{30,31} the s level is shifted downwards by 0.35 Ry (no shift is needed for p levels) and the exchange splitting is increased by 0.017 Ry; this fit was previously used in Ref.

32 in the calculations of exchange stiffness. We follow the fit of Ref. 32 by noting further that due to the reduced symmetry in the monolayer the d orbitals are subject to a significant crystal-field splitting, much greater than in the bulk. We characterize this crystal-field splitting with one parameter Δ_{cr} which is the difference between the energy of the out-of-plane orbitals ($yz, zx, 3z^2 - r^2$) and that of the in-plane orbitals ($xy, x^2 - y^2$). The value of Δ_{cr} was fitted to the energy bands of Refs. 30 and 31 to be around 0.01 Ry, which agrees with the estimate of Jepsen, Madsen, and Andersen³⁰ who found that the crystal splitting of the d orbitals is less than 0.015 Ry in the considered (001) fcc nickel monolayer. These values are several times smaller than those assumed in the calculations of anisotropy constants presented in Refs. 22 and 23. The final tight-binding fit to Refs. 30 and 31 for the energy bands of the nickel monolayer is, surprisingly, almost as accurate as in the original bulk fit. On the other hand, if we start from the Papaconstantopoulos's²⁹ bulk parameters in the *non-orthogonal* scheme, which leads to the more accurate energy bands in the bulk, we arrive at a rather poor approximation of the energy bands in the monolayer, although the required s -level shift is much smaller.

In the calculations with the d orbitals only, we assume the canonical two-center parameters^{30,33-36}

$$dd(\sigma, \pi, \delta) = (-6, 4, -1) \frac{W}{2.5} \left(\frac{s}{R} \right)^5, \quad (16)$$

where

$$W = 25(\mu_d s^2)^{-1} [\text{Ry}] \quad (17)$$

sets the energy scale (W is close to the bulk band width), s is the Wigner-Seitz radius, R the interatomic distance, and μ_d the effective d -band mass. The values of μ_d for various metals are given in Ref. 33; taking $\mu_d = 13$ for nickel,³⁰ we obtain $W = 3.9$ eV. The position of the Fermi energy ϵ_F in the d -orbitals-only case is chosen to give the correct magnitude of the magnetic moment M in the monolayer; for our nickel monolayer we take $M = 0.95\mu_B$ found in the *ab initio* calculations by Jepsen, Madsen, and Andersen.³⁰ From those calculations we also deduce that the exchange splitting Δ_{ex} is 1 eV. However, its accurate value is not important since for a strong ferromagnet, which is the case for nickel, K_{anis} is very insensitive to Δ_{ex} . This is quite obvious since according to formulas (14), (9), and (10), the largest contribution to K_{anis} should come from the vicinity of the Fermi level ϵ_F which does not cross the majority band in a strong ferromagnet.

The anisotropy constants K_{anis} calculated for various values of Δ_{cr} within both tight-binding schemes discussed above are presented in Fig. 1; we assume $\xi = 0.105$ eV (Ref. 36) in these calculations. As already established by Bruno²³ the crystal-field splitting has a large effect on the anisotropy constant K_{anis} . The general trend is similar for both the curves presented in Fig. 1, which suggests that the sp - d hybridization does not play the crucial role in determining K_{anis} . The differences arise from the different tight-binding energies and the different d com-

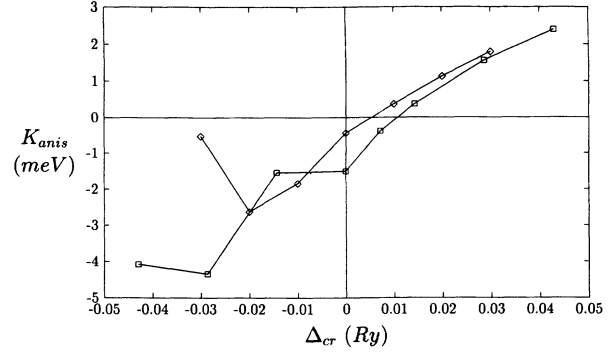


FIG. 1. The anisotropy constant K_{anis} (per atom) vs the crystal splitting Δ_{cr} for the (001) fcc nickel monolayer in the spd (\diamond) and the d -only canonical (\square) tight-binding schemes.

ponents of the corresponding eigenstates; the s and p orbitals present in the sum in Eq. (14) give a negligible contribution (less than 1.5%) to K_{anis} in the full spd scheme. The value of K_{anis} for the actual $\Delta_{\text{cr}} = 0.01$ Ry is positive (equal to 0.37 meV in the spd scheme). This means that the energy (7) of the (001) fcc nickel monolayer has its minimum for $\theta = \pi/2$, i.e., the magnetic moment lies in the plane of the monolayer.

B. Ferromagnetic slabs

Encouraged by the results for the monolayer, in the slabs we neglect the sp - d hybridization and use the canonical parameters [(16) and (17)]. While for nickel we take, as previously, $W = 3.9$ eV, for the two other ferromagnetic metals, cobalt and iron, we find $W = 4.4$ eV and $W = 4.9$ eV, respectively, from the values of μ_d given in Ref. 33. The magnetic moment M_{surf} of an atom in each of the two surface layers of the slab is enhanced with respect to that in the interior, M_{int} . We adopt the values of M_{surf} and M_{int} found in the *ab initio* calculations for the seven- and nine-layer slabs: $M_{\text{surf}} = 0.68\mu_B$, $M_{\text{int}} = 0.56\mu_B$ for nickel,³⁷ $M_{\text{surf}} = 1.86\mu_B$, $M_{\text{int}} = 1.65\mu_B$ for cobalt,³⁸ and $M_{\text{surf}} = 2.98\mu_B$, $M_{\text{int}} = 2.25\mu_B$ for iron,³⁹ as M_{int} we take the magnetic moment of an atom in the central layer. Here, we assume that the magnetic moment deviates from its bulk value only in the surface layer. This assumption is quite accurate.^{30,31,37-40} Moreover the *ab initio* values of the layer-projected magnetic moments are known only for slabs with a few layers, while our objective is to study slabs of arbitrary thickness and the effect of thickness on the magnetic anisotropy. To find the exchange splitting $\Delta_{\text{ex}}^{(l)}$ in the l th layer we assume that $\Delta_{\text{ex}}^{(l)}$ is proportional to the magnetic moment $M^{(l)}$ in this layer. This well-known property is a good approximation as it can be observed, for example, by comparing the ratio $U_{\text{ex}} = \Delta_{\text{ex}}/M = 1.05$ eV for the (001) nickel monolayer with the corresponding value $U_{\text{ex}} = 1.09$ eV obtained for bulk nickel [$\Delta_{\text{ex}} = 0.63$ eV, $M = 0.58\mu_B$ (Ref. 41)]. Thus in the case of nickel we take $U_{\text{ex}} = 0.275W$. From the *ab initio* calculations for bulk cobalt and iron we find correspondingly

$U_{\text{ex}}=0.26W$ [$\Delta_{\text{ex}}=1.8$ eV, $M=1.56\mu_B$ (Ref. 42)], and $U_{\text{ex}}=0.205W$ [$\Delta_{\text{ex}}=2.18$ eV, $M=2.16\mu_B$ (Ref. 43)]. To make the layer-projected magnetic moments

$$M^{(l)} = \frac{1}{N} \sum_{n\mathbf{k}\mu} |\langle \mathbf{k}l\mu\uparrow | n\mathbf{k}\uparrow \rangle|^2 \eta[\epsilon_F - \epsilon_{n\uparrow}(\mathbf{k})] - \frac{1}{N} \sum_{n\mathbf{k}\mu} |\langle \mathbf{k}l\mu\downarrow | n\mathbf{k}\downarrow \rangle|^2 \eta[\epsilon_F - \epsilon_{n\downarrow}(\mathbf{k})] \quad (18)$$

equal to the assumed values (i.e., M_{surf} in the surface layer, M_{int} elsewhere), one has to shift the d -orbital energies, by a certain amount $\delta\epsilon_d^{(l)}$, in each layer (with respect to those in the central layer); simultaneously one finds ϵ_F . These necessary shifts, found also in the *ab initio* calculations,^{37,44–45} can be understood as associated with the d -band narrowing at the surface due to the reduced coordination. In Eq. (18), N is the number of \mathbf{k} points in the two-dimensional zone sum.

As in the case of the nickel monolayer, an important role in the calculations of the magnetic anisotropy of the slabs, is played by the additional crystal splitting Δ_{cr} between the out-of-plane and the in-plane d orbitals. We assume that this splitting is present only in the outermost, surface layer. Since its value is rather uncertain, though expected to be positive, we take $\Delta_{\text{cr}}=0.05W$, a value similar to that found for the nickel monolayer.

The plots of K_{anis} vs the slab thickness L are presented in Figs. 2, 3, and 4; the values of K_{anis} were calculated with $\xi=0.105$ eV for nickel, $\xi=0.085$ eV for cobalt, and $\xi=0.075$ eV for iron.³⁶ The results for the monolayers, also shown in these figures, were obtained using the following magnetic moments: $M=0.95\mu_B$ for nickel,³⁰ $M=2.20\mu_B$ for cobalt,¹⁵ and $M=3.20\mu_B$ for iron.^{14,15,46} For each metal, K_{anis} has a well-defined sign. However, its magnitude fluctuates with the slab thickness, and these fluctuations do not settle down even for slabs as thick as 17 layers. Calculations for thicker slabs were not performed because of the very long computation time needed (e.g., more than 150 h on a fast alpha-processor

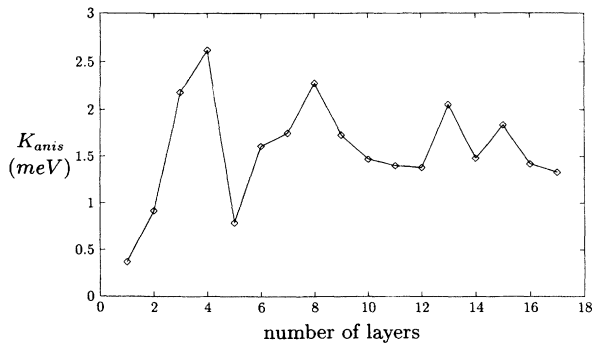


FIG. 2. The anisotropy constant K_{anis} (per unit surface cell) vs the number of layers for the (001) fcc nickel slab in the d -only canonical tight-binding scheme.

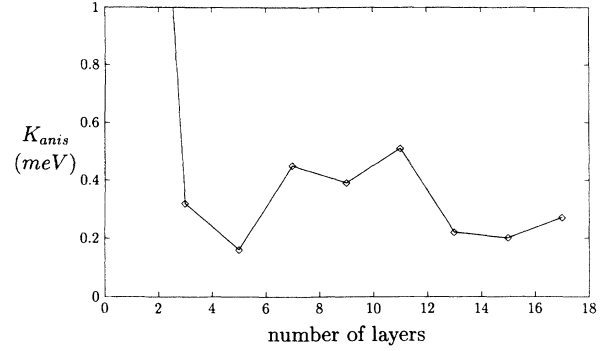


FIG. 3. The anisotropy constant K_{anis} (per unit surface cell) vs the number of layers for the (001) fcc cobalt slab in the d -only canonical tight-binding scheme. For the Co monolayer $K_{\text{anis}}=3.38$ meV is off scale.

DEC 3000/400 workstation), even if one takes into account that for thicker slabs the number of \mathbf{k} points in the Brillouin zone required to achieve 1–2 % accuracy of K_{anis} may be lowered to 30×30 , from 100×100 needed for the monolayer.

The observed fluctuations suggest that the contributions to the anisotropy constant K_{anis} come from several layers, not only from the surface one. This is also well seen in Table III, where we tried to separate these contributions to a certain extent. On the other hand, K_{anis} should be regarded as a quantity associated with the surface: it does not grow, on average, with the slab thickness L , as does the isotropic part of energy, K_0 , which shows a near to linear growth with L (cf. Fig. 5). We would also like to mention that the many-layer contributions to K_{anis} are observed even when all the layers except the surface one are made nonmagnetic (i.e., $M^{(l)}=0$, $l=2, \dots, L-1$) unless their layer-projected densities of states are arbitrarily pushed (almost) entirely below ϵ_F by a suitable shift of the d -orbital energies for the nonmagnetic layers.

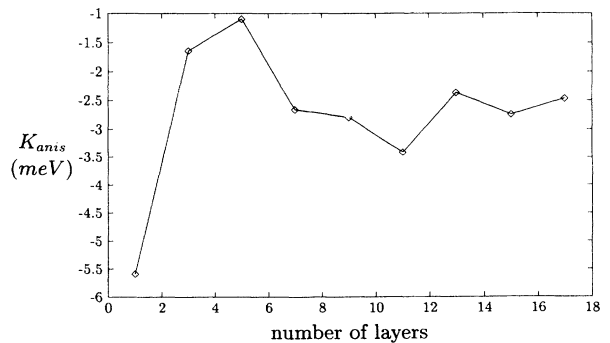


FIG. 4. The anisotropy constant K_{anis} (per unit surface cell) vs the number of layers for the (001) bcc iron slab in the d -only canonical tight-binding scheme.

TABLE III. The “partial” anisotropy constants $K^{(l_m)}$ obtained (analogously as K_{anis}) from Eqs. (14), (9), and (10) with the summation layer indices l, l' restricted to range $1 \leq l, l' \leq l_m$ for the 17-layer (001) fcc nickel slab in the d -only canonical tight-binding scheme.

l_m	1	2	3	4	5	6	7	8	9	10	11	12	13	14	15	16	17
$K^{(l_m)}$ (meV)	0.85	0.78	0.62	0.76	0.65	0.51	0.57	0.47	0.43	0.43	0.41	0.36	0.49	0.54	0.33	0.49	1.33

IV. DISCUSSION

The signs of the anisotropy constants obtained for the Ni, Co, and Fe monolayers agree with those found in the recent *ab initio* calculations^{14,15,18–20} (except Ref. 16 where a very small *positive* K_{anis} is predicted for iron), and also with the results of a different tight-binding scheme.²³ These signs do not change for the several-layer slabs; let us note here also that we do not observe the different behavior of K_{anis} for the even and the odd number of layers which was predicted in an earlier work by Bennett;²¹ cf. Fig. 2. Thus we come to the conclusion that while the Ni and Co slabs are magnetized in-plane, the Fe slabs may have the magnetization perpendicular to the slab. These predictions are in agreement with the experimental data.^{5,9–12} In particular, $\frac{1}{2}K_{\text{anis}} = 0.15–0.3$ meV calculated for cobalt slabs (with $L \geq 2$) agrees reasonably well with the value 0.41 ± 0.07 meV determined experimentally for the anisotropy constant of a single Co/vacuum interface.¹²

To investigate fully the case of iron, we also calculated the additional anisotropy term, K_{dip} , to be added to our anisotropy constant, arising from the magnetostatic interaction between the magnetic moments (dipole-dipole interaction):

$$K_{\text{dip}} = \frac{3}{4} \sum_{ll'} \frac{M^{(l)}M^{(l')}}{[(\mathbf{R}_j^{(l')} - \mathbf{R}_0^{(l)})^2 + (z^{(l')} - z^{(l)})^2]^{3/2}} \times \left\{ 1 - 3 \frac{(z^{(l')} - z^{(l)})^2}{(\mathbf{R}_j^{(l')} - \mathbf{R}_0^{(l)})^2 + (z^{(l')} - z^{(l)})^2} \right\} \quad (19)$$

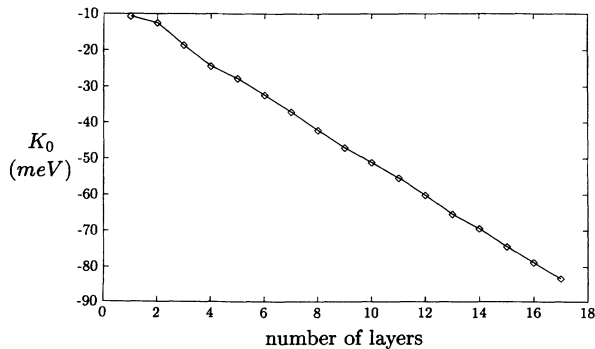


FIG. 5. The isotropic part of energy K_0 (per unit surface cell) vs the number of layers for the (001) fcc nickel slab in the d -only canonical tight-binding scheme.

(the shape anisotropy constant per unit surface cell). The expression (19) is valid for slabs with a fourfold symmetry axis perpendicular to the slab surface, which is the case for (001) bcc iron slabs considered. The value of K_{dip} is positive, so it favors the in-plane magnetization, and it is roughly proportional to the slab thickness. The total anisotropy constant, $K_{\text{anis}} + K_{\text{dip}}$, for iron slabs is shown in Fig. 6; as is seen, it is negative for $L < 17$. In experiment the perpendicular magnetic moment was observed for iron slabs with $L < 7$.⁶ This means that the values of K_{anis} obtained are too large though they have the correct sign. On the other hand, in an earlier work¹⁵ the sum $K_{\text{anis}} + K_{\text{dip}}$ was negative only for the one-layer iron slab, so the values of K_{anis} were too small.

APPENDIX

The triangular method⁴⁷ is the two-dimensional analog of the well-known tetrahedron method⁴⁸ used for three-dimensional \mathbf{k} -space integrations. First, the two-dimensional \mathbf{k} space is divided into elementary triangles and the energies $\epsilon_{n\sigma}(\mathbf{k})$ are interpolated linearly within each triangle (on the basis of their values in the corners of the triangles), while $a_{n,l\mu}^\sigma(\mathbf{k})$ is assumed to be constant in the triangle. Then, for each triangle its part where the factor $\eta[\epsilon_{n''\sigma''}(\mathbf{k}) - \epsilon_F]\eta[\epsilon_F - \epsilon_{n'\sigma'}(\mathbf{k})]$ [appearing in Eq. (10)] is nonzero (equal to 1), is either a triangle or a sum of triangles. Within each of these resulting triangles the sum $\sum_{\mathbf{k}} [\epsilon_{n''\sigma''}(\mathbf{k}) - \epsilon_{n'\sigma'}(\mathbf{k})]^{-1}$ can be performed analytically in the infinitely dense \mathbf{k} -mesh limit:

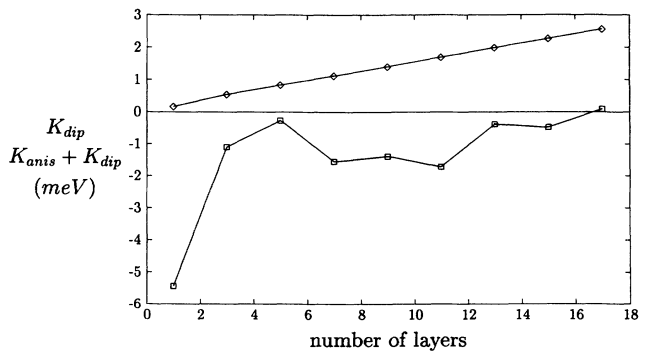


FIG. 6. The shape anisotropy constant K_{dip} (\diamond) and the total anisotropy constant $K_{\text{anis}} + K_{\text{dip}}$ (\square) (per unit surface cell) vs the number of layers for the (001) bcc iron slab in the d -only canonical tight-binding scheme.

$$\int_{\text{triangle}} \frac{1}{\epsilon_{n''\sigma''}(\mathbf{k}) - \epsilon_{n'\sigma'}(\mathbf{k})} d\mathbf{k}$$

$$= 2S_{\text{triangle}} \left[\frac{\Delta_1 \ln|\Delta_1|}{(\Delta_1 - \Delta_2)(\Delta_1 - \Delta_3)} + \frac{\Delta_2 \ln|\Delta_2|}{(\Delta_2 - \Delta_1)(\Delta_2 - \Delta_3)} + \frac{\Delta_3 \ln|\Delta_3|}{(\Delta_3 - \Delta_1)(\Delta_3 - \Delta_2)} \right], \quad (20)$$

where S_{triangle} is the surface of the triangle $(\mathbf{k}_1, \mathbf{k}_2, \mathbf{k}_3)$, while $\Delta_i = \epsilon_{n''\sigma''}(\mathbf{k}_i) - \epsilon_{n'\sigma'}(\mathbf{k}_i)$, $i = 1, 2, 3$.

ACKNOWLEDGMENTS

One of us (M.C.) would like to thank the Royal Society for financing his stay at Imperial College.

*Permanent address: Institute of Physical Chemistry of the Polish Academy of Sciences, ul. Kasprzaka 44/52, 01-224 Warszawa, Poland.

- ¹M. L. Néel, *J. Phys. Radium* **15**, 225 (1954).
²P. F. Carcia, A. D. Meinhardt, and A. Suna, *Appl. Phys. Lett.* **47**, 178 (1985).
³C. Chappert, K. Le Dang, P. Beauvillain, H. Hurdequint, and D. Renard, *Phys. Rev. B* **34**, 3192 (1986).
⁴H. J. G. Draaisma, W. J. M. de Jonge, and F. J. A. den Broeder, *J. Magn. Magn. Mater.* **66**, 351 (1987).
⁵D. Pescia, G. Zampieri, M. Stampanoni, G. L. Bona, R. F. Willis, and F. Meier, *Phys. Rev. Lett.* **58**, 933 (1987).
⁶B. Heinrich, J. F. Cochran, A. S. Arrot, S. T. Purcell, K. B. Urquhart, J. R. Dutcher, and W. F. Egelhoff, *J. Appl. Phys. A* **49**, 473 (1989).
⁷C. Liu and S. D. Bader, *J. Magn. Magn. Mater.* **93**, 307 (1991).
⁸H. Hurdequint, *J. Magn. Magn. Mater.* **93**, 336 (1991).
⁹J. Voigt, X. L. Ding, R. Fink, G. Krausch, B. Luckscheiter, R. Platzer, U. Wöhrmann, and G. Schatz, *J. Magn. Magn. Mater.* **93**, 341 (1991).
¹⁰F. J. A. den Broeder, W. Hoving, and P. J. H. Bloemen, *J. Magn. Magn. Mater.* **93**, 562 (1991).
¹¹M. T. Johnson, J. J. de Vries, N. W. E. McGee, J. ann de Stegge, and F. J. A. den Broeder, *Phys. Rev. Lett.* **69**, 3575 (1992).
¹²P. Krams, F. Lauks, R. L. Stamps, B. Hillebrands, and G. Güntherodt, *Phys. Rev. Lett.* **69**, 3674 (1992).
¹³J. H. Van Vleck, *Phys. Rev.* **52**, 1178 (1937).
¹⁴J. G. Gay and R. Richter, *Phys. Rev. Lett.* **56**, 2728 (1986).
¹⁵J. G. Gay and R. Richter, *J. Appl. Phys.* **61**, 3362 (1987).
¹⁶Chun Li, A. J. Freeman, H. J. F. Jansen, and C. L. Fu, *Phys. Rev.* **42**, 5433 (1990).
¹⁷A. J. Freeman and Chun Li, *J. Appl. Phys.* **69**, 5215 (1991).
¹⁸G. Y. Guo, W. M. Temmerman, and H. Ebert, *J. Phys. Condens. Matter* **3**, 8205 (1991).
¹⁹G. H. O. Daalderop, Ph.D. thesis, Technische Universiteit Delft, 1991.
²⁰Ding-sheng Wang, Ruqian Wu, and A. J. Freeman, *Phys. Rev. Lett.* **70**, 869 (1993).
²¹A. J. Bennett and B. R. Cooper, *Phys. Rev. B* **3**, 1642 (1971).
²²H. Takayama, K.-P. Bohnen, and P. Fulde, *Phys. Rev. B* **14**, 2287 (1976).
²³P. Bruno, *Phys. Rev. B* **39**, 865 (1989).
²⁴J. C. Slater and G. F. Koster, *Phys. Rev.* **94**, 1498 (1954).
²⁵W. A. Harrison, *Electronic Structure and the Properties of Solids* (Freeman, San Francisco, 1980).
²⁶E. Abate and M. Asdente, *Phys. Rev.* **140**, A1303 (1965).
²⁷H. Brooks, *Phys. Rev.* **58**, 909 (1940).
²⁸P. Bruno, Ph.D. thesis, Université de Paris-Sud, 1989.
²⁹D. A. Papaconstantopoulos, *Handbook of the Band Structure of Elemental Solids* (Plenum, New York, 1986).
³⁰O. Jepsen, J. Madsen, and O. K. Andersen, *Phys. Rev. B* **26**, 2790 (1982).
³¹Xue-yuan Zhu and J. Hermanson, *Phys. Rev. B* **27**, 2092 (1983).
³²J. d'Albuquerque e Castro, D. M. Edwards, J. Mathon, and R. B. Muniz, *J. Magn. Magn. Mater.* **93**, 295 (1991).
³³O. K. Andersen and O. Jepsen, *Physica* **91B**, 317 (1977).
³⁴D. G. Pettifor, *J. Phys. F* **7**, 613 (1977).
³⁵O. K. Andersen, W. Klose, and H. Nohl, *Phys. Rev. B* **17**, 1209 (1978).
³⁶A. R. Mackintosh and O. K. Andersen, in *Electrons at the Fermi Surface*, edited by M. Springford (Cambridge University Press, Cambridge, 1980).
³⁷E. Wimmer, A. J. Freeman, and H. Krakauer, *Phys. Rev. B* **30**, 3113 (1984).
³⁸Chun Li, A. J. Freeman, and C. L. Fu, *J. Magn. Magn. Mater.* **75**, 53 (1988).
³⁹S. Ohnishi, A. J. Freeman, and M. Weinert, *Phys. Rev. B* **28**, 6741 (1983).
⁴⁰M. Aldén, S. Mirbt, H. L. Skriver, N. M. Rosengaard, and B. Johansson, *Phys. Rev. B* **46**, 6303 (1992).
⁴¹C. S. Wang and J. Callaway, *Phys. Rev. B* **15**, 298 (1977).
⁴²V. L. Moruzzi, J. F. Janak, and A. R. Williams, *Calculated Electronic Properties of Metals* (Pergamon, New York, 1978).
⁴³J. Callaway and C. S. Wang, *Phys. Rev. B* **16**, 2095 (1977).
⁴⁴H. Krakauer, A. J. Freeman, and E. Wimmer, *Phys. Rev. B* **28**, 610 (1983).
⁴⁵Xue-yuan Zhu, J. Hermanson, F. J. Arlinghaus, J. G. Gay, R. Richter, and J. R. Smith, *Phys. Rev. B* **29**, 4426 (1984).
⁴⁶C. L. Fu, A. J. Freeman, and T. Oguchi, *Phys. Rev. Lett.* **54**, 2700 (1985).
⁴⁷O. Jepsen, J. Madsen, and O. K. Andersen, *Phys. Rev. B* **18**, 605 (1978).
⁴⁸J. Rath and A. J. Freeman, *Phys. Rev. B* **11**, 2109 (1975).